Theory of Catalysis

DOI: 10.1002/anie.201402115

Computational Kinetics of Cobalt-Catalyzed Alkene Hydroformylation**

*Laura E. Rush, Paul G. Pringle, and Jeremy N. Harvey**

Dedicated to the MPI für Kohlenforschung on the occasion of its centenary

Abstract: *Density functional theory, coupled-cluster theory, and transition state theory are used to build a computational model of the kinetics of phosphine-free cobalt-catalyzed hydroformylation and hydrogenation of alkenes. The model provides very good agreement with experiment, and enables the factors that determine the selectivity and rate of catalysis to be determined. The turnover rate is mainly determined by the alkene coordination step.*

Cobalt-catalyzed hydroformylation, which was discovered 75 years ago based on earlier work at the Max Planck Institute for Coal Research, is the first reported metal-complex-catalyzed industrial process.[1] Though rhodium catalysts have largely superseded cobalt systems because of greater efficiency, cobalt catalysts are cheaper, less toxic, and more thermally stable, and continue to be used.[2,3] Thus there continues to be much interest in the development of modified cobalt catalysts with increased activity, longevity, regioselectivity, and chemoselectivity especially with respect to avoiding wasteful alkene substrate hydrogenation. For each of these aspects of catalyst improvement, a detailed understanding of the hydroformylation mechanism is pivotal.

Based on the mechanistic work of Heck and Breslow[4] and subsequent studies,[5] the hydroformylation mechanism with both rhodium and cobalt systems is quite well understood. Intermediates such as cobalt acyl tetracarbonyls [$RCOCo(CO)_4$] or phosphine derivatives thereof [$RCOCo(CO)_3L$] (where $L = PR_3$) have been detected under catalytic conditions,[4,6] and their reactivity studied.[7] The reactivity of the corresponding unsaturated intermediate [$RCOCo(CO)_2L$] obtained by flash photolysis has also been carefully examined.[8] Kinetics are available, in particular a systematic study[9] of the rate of hydroformylation of propene by [$HCo(CO)_4$], which gave the following empirical rate law:

$$\frac{-d[CO]}{dt} = k\frac{[H_2]^{0.6}[CO][Cat]^{0.8}[Alkene]}{(1+K[CO])^2} \quad (1)$$

The non-integer orders with respect to total initial concentration of catalyst [Cat] and to concentration of hydrogen indicate a complex underlying mechanism that was not resolved in this kinetic study. Indeed, despite the extensive work, there is no consensus concerning the nature of the turnover limiting step.

The hydroformylation reaction with cobalt[10] and rhodium[11] catalysts has also been the subject of many computational studies, which have addressed aspects such as the structure of intermediates, the detailed mechanism of each elementary step, and the effect of phosphine ligands on reactivity. While these studies have confirmed the mechanistic picture emerging from the experimental studies, an unequivocal identification of the turnover-limiting step in the cobalt-catalyzed reaction remains elusive. This is partly due to the fact that most of the previous work has used density functional theory (DFT), which is a relatively low accuracy method. Also, previous computational work has not included an exploration of the competing alkene hydrogenation.

In other fields such as combustion chemistry, it has been shown that computational kinetics models—based on accurate electronic structure theory and transition state theory (TST)—can greatly enhance the understanding of complex reacting systems.[12] In this study, we use a similar methodology to study phosphine-free cobalt-catalyzed hydroformylation and hydrogenation of propene. Our calculations use DFT and explicitly correlated coupled-cluster[13] electronic structure methods together with TST.[14]

The mechanism as obtained in our study is shown in Scheme 1, with calculated energies given in Table 1. In this first study, we have focused on the pathway leading to the major linear product. Many of the species in Scheme 1 have been described before,[10] so we will only provide a brief discussion of energies and structures, then emphasize the predicted kinetics at 150 °C, a typical temperature used for catalysis.

Hydroformylation is initiated from [$HCo(CO)_4$] **1** by loss of CO to yield the 16-electron species **2**, followed by addition of alkene **3**, to yield **4**. The unsaturated species **2** lies much higher in potential energy than **1** or **4**, and we could not find any barrier to the addition of CO or alkene, so that the corresponding transition states (TSs) are purely entropic in origin. Previous studies have assumed that substitution leading from **1** to **4** occurs through this dissociative mechanism. However, associative ligand substitution mechanisms can be favoured over dissociative mechanisms in other organometallic reactions.[15] Accordingly, we searched for

[*] L. E. Rush, Prof. Dr. P. G. Pringle, Prof. Dr. J. N. Harvey
School of Chemistry, University of Bristol
Cantock's Close, Bristol, BS8 1TS (UK)
E-mail: jeremy.harvey@bristol.ac.uk

[**] We thank the Bristol Chemical Synthesis Centre for Doctoral Training, funded by EPSRC (EP/G036764/1), and the University of Bristol, for a Ph.D. studentship (LR).

Supporting information for this article is available on the WWW under http://dx.doi.org/10.1002/anie.201402115.

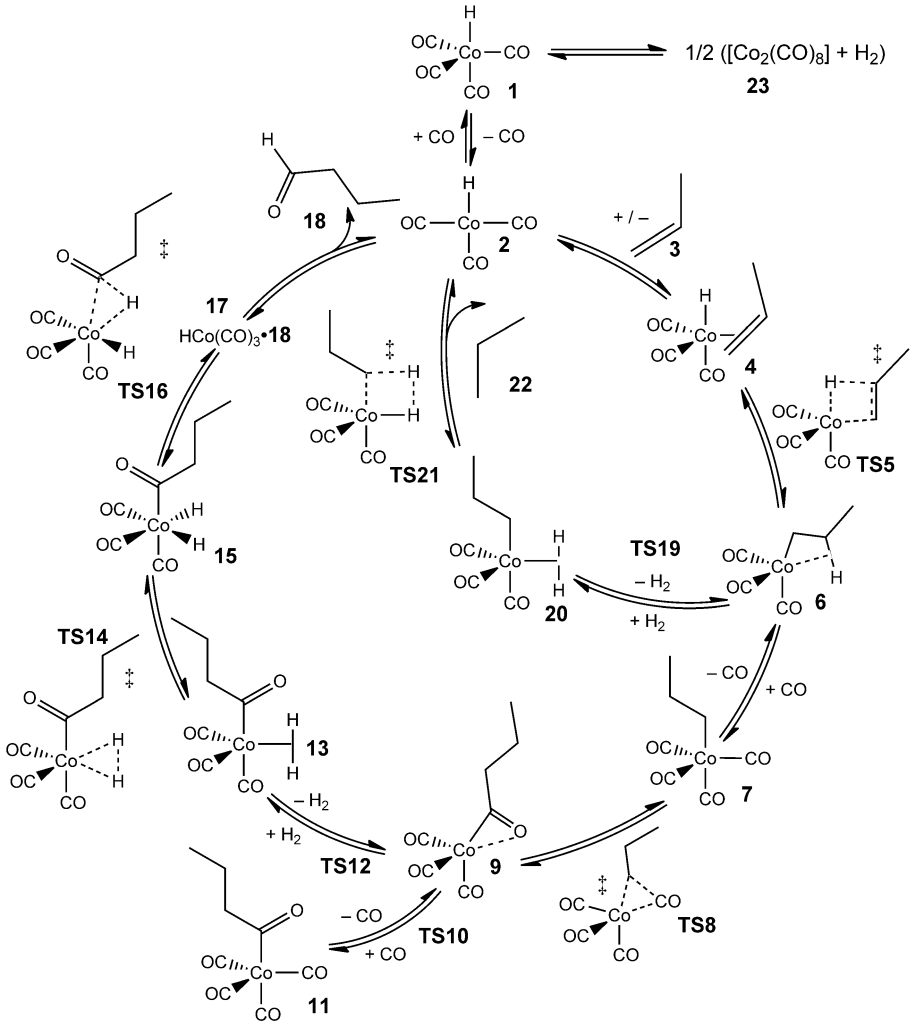

Scheme 1. Modeled catalytic cycle for alkene hydroformylation and hydrogenation.

TSs corresponding to such mechanisms, but could not locate any that would be competitive with the dissociative route.[16]

The next steps in the mechanism are insertion of the alkene into the Co–H bond of **4** through **TS5** to yield the 16-electron ethyl complex **6**, which can add carbon monoxide (without a potential energy barrier) to form the corresponding tetracarbonyl species **7**. This can in turn undergo CO insertion into the cobalt–alkyl bond through **TS8** to yield an unsaturated acyl species **9**. Addition of carbon monoxide to **9** involves a small potential energy barrier, **TS10**, because of the need to "displace" the acyl oxygen atom that interacts with the formally vacant site at the metal. This process yields the saturated acylcobalt tetracarbonyl species **11**, the intermediate with the lowest potential energy in the whole catalytic cycle (though it lies higher in standard free energy at 150 °C than **7**). From this stable species, the first step towards the hydroformylation product is the reverse of the last process—loss of carbon monoxide to yield **9**, followed by addition of molecular hydrogen (over the low barrier **TS12**) leading to the dihydrogen complex **13**. Dihydrogen activation can then occur to yield the dihydride **15**, followed by reductive elimination to form a weakly bonded complex **17** between the product and $[HCo(CO)_3]$. Finally, to complete the formal catalytic cycle, this species can release the product and add carbon monoxide.

While the above cycle is described as starting from monomeric **1**, this species is known to be in (fairly rapid) equilibrium with $[Co_2(CO)_8]$ **23** under catalytic conditions. For this species CCSD(T) calculations are not possible (because of computational expense and multireference behavior) so our computed energy is based on DFT. The calculated free energy change of 30.6 kJ mol^{-1} for forming two equivalents of **1** from **23** and hydrogen is in good agreement with the experimental value measured in heptane (22.6 kJ mol^{-1}).[17]

Alkene hydrogenation is a wasteful side reaction in some applications of hydroformylation, but has not been considered in previous studies of the cobalt-catalyzed reaction.[10] We propose that it occurs from intermediate **6**, by addition of H_2 instead of CO, to yield the dihydrogen complex **20**, over a low barrier **TS19**. In contrast to the case of the related complex **13**, which yields product **18** through oxidative addition/reductive elimination, release of propane **22** is found to occur through a one-step σ-bond metathesis over **TS21**. This transition state has a structure somewhat similar to that of the reductive elimination **TS16** in the hydroformylation mechanism. The putative TS for oxidative addition of H_2 to **20** has apparently disappeared. It is noteworthy that the corresponding **TS14** lies lower in potential energy than the Co^{III} dihydride species **15**, perhaps because this species is a minimum at the B3LYP level of theory used for optimization, but not at the CCSD(T) level. Note that hydrogenation of the aldehyde product to form an alcohol also often occurs during hydroformylation (especially with phosphine-modified catalysts).[3] Exploring the mechanism and relative rate of this reaction would be valuable but goes beyond the scope of this study.

Based on our experience,[18] our CCSD(T)-F12 protocol should yield accurate energies for transition metal compounds, with an error of approximately 10 kJ mol^{-1}. The experimental room temperature enthalpy change for the hydrogenation and hydroformylation of propene are −123.9 and −109.9 kJ mol^{-1} respectively,[19] compared to calculated values of −122.9 and −108.4 kJ mol^{-1}.

Table 1: Computed relative energies and free energies at 150 °C for propene hydroformylation and hydrogenation [kJ mol^{-1}].

	ΔE_{rel}(CCSD(T))	ΔG_{rel}(CCSD(T))
1/2 **23** + **3** + 3/2 H_2 + CO	−23.0[a]	−15.3[a]
1 + **3** + H_2 + CO	0.0	0.0
2 + **3** + H_2 + 2 CO	148.0	84.7
4 + H_2 + 2 CO	35.1	33.2
TS5 + H_2 + 2 CO	62.3	59.3
6 + H_2 + 2 CO	39.5	35.8
7 + H_2 + CO	−46.0	8.0
TS8 + H_2 + CO	12.2	65.8
9 + H_2 + CO	−0.9	48.3
TS10 + H_2	2.5	103.1
11 + H_2	−88.6	21.1
TS12 + CO	19.3	108.6
13 + CO	−6.2	89.9
TS14 + CO	9.9	102.6
15 + CO	13.1	110.1
TS16 + CO	24.7	123.0
17 + CO	−14.2	73.2
2 + **18** + CO	49.8	88.9
1 + **18**	−98.2	4.2
TS19 + 2 CO	74.3	103.6
20 + 2 CO	41.7	80.0
TS21 + 2 CO	86.4	123.8
1 + **22** + CO	−116.4	−70.0

[a] Value for $Co_2(CO)_8$ obtained at the B3LYP-D3 level.

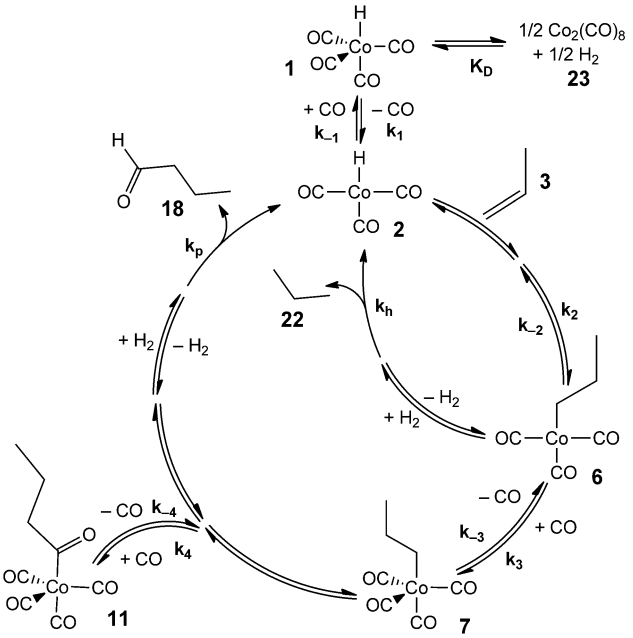

Scheme 2. Reduced mechanism for hydroformylation.

We now consider the predicted kinetic behavior. Traditionally such considerations have been a minor part of computational studies of catalysis, but there has been a growing realization that deducing a mechanism solely from relative free energies is not always straightforward. Hence protocols for interpreting free-energy profiles have been suggested,[20] and the value of kinetic simulations for understanding mechanisms is becoming increasingly recognized.[21] We use TST to predict rate constants based on the calculated activation free energies. Differences in free energy between stable species, also computed from the ab initio data (except for the equilibrium with **23** where we do not have CCSD(T) values and base our calculations on experiment[17] rather than the less accurate DFT value), are used to compute equilibrium constants.

For reactions proceeding without a barrier on the potential energy surface, the rate constants are estimated, as in previous work.[16c] They are assumed to be diffusion-controlled, with rate constants in solution given by the approximate expression $k = 8k_BT/3\eta$, where k_B is Boltzmann's constant, T is temperature, and η is the solvent viscosity.[22] For toluene at 150 °C and 100 bar, η is 2.09×10^{-4} Pa s,[23] yielding a diffusion-controlled rate constant of 4.49×10^{10} M^{-1} s^{-1} at 150 °C.

The modeled mechanism of Scheme 1 contains many elementary steps. For the kinetic analysis, we have assumed that some processes with low barriers are in quasi-equilibrium throughout. This enabled us to combine their equilibrium constants with rate constants for other steps, in the spirit of the Curtin–Hammett principle. We also assumed that the reductive elimination steps leading to aldehyde or alkane are irreversible under catalytic conditions—hence we only included the forward rate constants k_h and k_p. Upon using this simplification, we obtained the reduced mechanism shown in Scheme 2. The steady-state approximation was then applied to the concentrations of each of the cobalt-containing species. The concentrations or partial pressures of all other species (alkene, hydrogen, solvent, and carbon monoxide) were assumed not to change. The set of steady-state kinetic equations was solved to yield an expression for the rate of catalysis R (or rate of production of **18**) as a function of the concentrations of **1** and alkene, and the partial pressures of hydrogen p_{H2} and carbon monoxide p_{CO}:

$$R = \frac{k_p K_1 k_2 k_3 [\text{Alkene}] p_{H_2}}{k_{-2}k_{-3} + p_{H_2}\left(k_3 k_p p_{CO} + k_{-2}k_p + k_h k_{-3} + k_h k_p p_{H_2}\right)} [\mathbf{1}] \quad (2)$$

where k_p, k_2, k_3, k_{-2}, k_{-3}, and k_h are rate constants as shown in Scheme 2, and K_D and K_1 ($= k_1/k_{-1}$) are equilibrium constants. The concentration [**1**] is related to the total concentration of cobalt [Co], which is twice the nominal value of [**23**]:

$$[\mathbf{1}] = \frac{1}{4k_D}\left\{-p_{H_2}F + \sqrt{p_{H_2}^2F^2 + 8p_{H_2}K_D[\text{Co}]}\right\} \quad (3)$$

where $1/F$ is the fraction of monomeric cobalt species that are present as **1**, typically close to 100% for the conditions considered here. This is obtained from a complicated expression shown in the Supporting Information.

By using Equation (2), the rate for catalysis can be computed for the various sets of concentrations where rates have been measured.[9] Comparison of theoretical and experimental rates is shown in Figure 1 and the Supporting Information. Given that no fitting to experiment has been carried out, and the exponential dependence of rates on

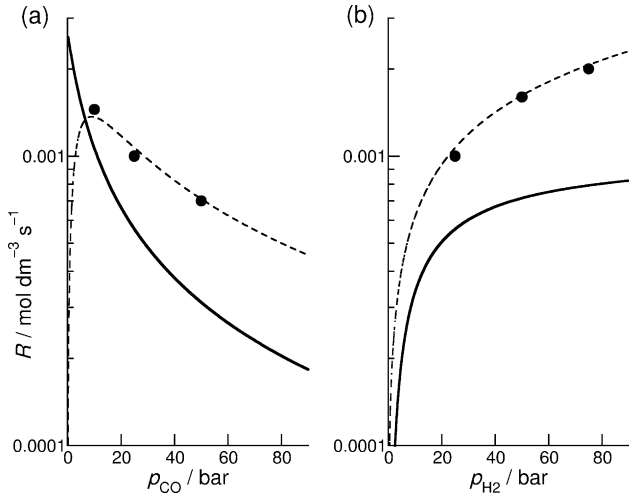

Figure 1. Rates of hydroformylation of propene at 150 °C. Experimental (dots); values from the fit to experiment of Equation (1) (dashed line); values computed according to Equation (2) (solid line). [Co] is 1.46×10^{-2} mol dm^{-3}, [propene] is 1.19 mol dm^{-3}. a) Rate as a function of p_{CO}, with $p_{H_2}=25$ bar; b) rate as a function of p_{H_2}, with $p_{CO}=25$ bar.

relative free energies, it would be surprising if a perfect match to experiment was obtained—and in fact the calculated rates differ from the experimental values by roughly a factor of two. However, the agreement between experiment and theory is very good for the shape of the curves of R as a function of p_{CO}, p_{H_2}, [Co], and [Alkene], implying that the overall order of reaction is well-described. Also, a factor of two is perhaps even better than can be expected for such theory–experiment comparisons, since it implies that the key relative free energies at 150 °C are accurate to better than 3 kJ mol^{-1}. This degree of agreement must be in part fortuitous. As shown in the Supporting Information, a slight adjustment (6 kJ mol^{-1} or less) to just three of the relative free energies in Table 1 leads to an improved theoretical model that reproduces experimental rates quantitatively. It has been found in other computational kinetics studies[12] that such adjustments (by less than the error of the computational method) can lead to useful predictive models.

The relation between the empirical rate law of Equation (1) and the theoretical expression of Equation (2) is not immediately obvious, though clearly they give similar behavior, as shown in Figure 1. It is possible to derive a simplified form of Equation (2) upon neglecting some smaller terms, and this helps to understand the link to Equation (1) and also to identify the elementary step that is closest to being turnover-limiting. As shown in Table S2 in the Supporting Information, F is typically close to 1, and for low p_{H2} and high [Co], Equation (3) can be simplified to:

$$[\mathbf{1}] \approx \sqrt{\frac{p_{H_2}[\mathrm{Co}]}{2K_D}} \tag{4}$$

Also, the first term within parentheses in the denominator of Equation (2) is the largest for typical conditions. If one considers only this term, and uses the simplified Equation (4), then Equation (2) reduces to:

$$R \approx \frac{K_1 k_2}{(2K_D)^{1/2}} \times \frac{p_{H_2}^{1/2}[\mathrm{Co}]^{1/2}[\mathrm{Alkene}]}{p_{CO}} \tag{5}$$

This is much more similar to Equation (1), especially considering that the second term in the denominator of Equation (1) is much larger than the first term except at very low p_{CO} values, when low turnover is found experimentally because of catalyst decomposition, which is not modeled in our mechanism of Scheme 1. Equation (5) provides insight into the turnover-limiting step. For low p_{H2} values, most of the cobalt is predicted to be present as unreactive dimer **23**, with the concentration of **1** rising only with the square root of the total [Co] and p_{H2} values, because of the equilibrium between these species.[24] The unsaturated **2** is present in minute amounts, in equilibrium with **1**, and its concentration is suppressed as p_{CO} increases. Despite its large rate constant, the turnover-limiting step is the addition of alkene to **2**, because of the very low concentration of this very active species. This description accounts for the form of Equation (5) and for the qualitative behavior of the rate as a function of p_{CO}, p_{H_2}, [Alkene], and [Co]. The detailed Equation (2) is however needed to make quantitative predictions.

The model also provides an expression for the rate of alkene hydrogenation, as shown in the Supporting Information. As shown in Table 1, **TS16** (leading to hydroformylation) and **TS21** (leading to hydrogenation) are very close in standard free energy at 150 °C, so one might expect hydrogenation to compete very effectively with hydroformylation. However, starting from species **6**, the rate for hydroformylation increases with p_{CO}, whereas that for hydrogenation does not, so that under catalytic conditions with large p_{CO}, hydroformylation is predicted by the present model to predominate, with a selectivity of around 98 % (consistent with a yield of alkane of 2 % mentioned in Ref. [3]). For low p_{CO} values, though, hydrogenation becomes increasingly competitive—for example, for $p_{CO}=10$ bar in Figure 1 the calculations suggest that the selectivity is only of 92 % towards hydroformylation.

In summary, our computational kinetics approach provides a detailed bottom-up model of alkene hydroformylation using phosphine-free cobalt catalysis. While many important aspects are not yet included (e.g., ligand effects, aldehyde hydrogenation, and regioselectivity), very good agreement is obtained between the experimentally observed and the theoretically predicted rates, considering the high sensitivity of calculated rates to relative electronic energies. This is no doubt due to both the high accuracy of the explicitly correlated CCSD(T)-F12 method as well as to some error cancellation. In the spirit of computational kinetics, slight adjustments to the underlying ab initio parameters provide a quantitatively predictive model. Our calculations suggest that turnover is mainly limited by the step in which alkene adds to the coordinatively unsaturated [HCo(CO)$_3$] species **2**, despite the fact that this step does not have a potential energy barrier. Also, we study here the competing hydrogenation process, and show that it is competitive with hydroformylation at low p_{CO} values.

Received: February 5, 2014
Published online: April 3, 2014

Keywords: cobalt · density functional calculations · homogeneous catalysis · hydroformylation · reaction kinetics

[1] O. Roelen, German Patent, DE 849548, **1938**; B. Cornils, W. A. Herrmann, M. Rasch, *Angew. Chem.* **1994**, *106*, 2219 – 2238.

[2] L. T. Mika, L. Orha, E. Driessche, R. Garton, K. Zih-Perenyi, I. T. Horvath, *Organometallics* **2013**, *32*, 5326 – 5332; P. N. Bungu, S. Otto, *Dalton Trans.* **2007**, 2876 – 2884; J. M. Birbeck, A. Haynes, H. Adams, L. Damoense, S. Otto, *ACS Catal.* **2012**, *2*, 2512 – 2523; C. Godard, S. B. Duckett, S. Polas, R. Tooze, A. C. Whitwood, *Dalton Trans.* **2009**, 2496 – 2509; L. Damoense, M. Datt, M. Green, C. Steenkamp, *Coord. Chem. Rev.* **2004**, *248*, 2393 – 2407; C. Dwyer, H. Assumption, J. Coetzee, C. Crause, L. Damoense, M. Kirk, *Coord. Chem. Rev.* **2004**, *248*, 653 – 669; P. N. Bungu, S. Otto, *Dalton Trans.* **2011**, *40*, 9238 – 9249; M. Carreira, M. Charernsuk, M. Eberhard, N. Fey, R. van Ginkel, A. Hamilton, W. P. Mul, A. G. Orpen, H. Phetmung, P. G. Pringle, *J. Am. Chem. Soc.* **2009**, *131*, 3078 – 3092.

[3] P. W. N. M. van Leeuwen, *Homogeneous Catalysis*, *Understanding the Art*, Kluwer, Dordrecht, **2004**.

[4] R. F. Heck, D. S. Breslow, *J. Am. Chem. Soc.* **1961**, *83*, 4023 – 4027; R. F. Heck, *Acc. Chem. Res.* **1969**, *2*, 10 – 16.

[5] F. Hebrard, P. Kalck, *Chem. Rev.* **2009**, *109*, 4272 – 4282; A. L. Watkins, C. R. Landis, *J. Am. Chem. Soc.* **2010**, *132*, 10306 – 10317.

[6] J. W. Rathke, R. J. Klingler, T. R. Krause, *Organometallics* **1991**, *10*, 1350 – 1355.

[7] I. Kovács, F. Ungváry, L. Markó, *Organometallics* **1986**, *5*, 209 – 215.

[8] S. M. Massick, T. Büttner, P. C. Ford, *Inorg. Chem.* **2003**, *42*, 575 – 580.

[9] R. V. Gholap, O. M. Kut, J. R. Bourne, *Ind. Eng. Chem. Res.* **1992**, *31*, 1597 – 1601.

[10] M. Torrent, M. Solà, G. Frenking, *Chem. Rev.* **2000**, *100*, 439 – 493; C.-F. Huo, Y.-W. Li, M. Beller, H. Jiao, *Organometallics* **2003**, *22*, 4665 – 4677; S. Maeda, K. Morokuma, *J. Chem. Theory Comput.* **2012**, *8*, 380 – 385.

[11] M. Sparta, K. J. Børve, V. R. Jensen, *J. Am. Chem. Soc.* **2007**, *129*, 8487 – 8499; M. À. Carvajal, S. Kozuch, S. Shaik, *Organometallics* **2009**, *28*, 3656 – 3665.

[12] J. Zádor, C. A. Taatjes, R. X. Fernandes, *Prog. Energy Combust. Sci.* **2011**, *37*, 371 – 421; A. Jalan, I. M. Alecu, R. Meana-Pañeda, J. Aguilera-Iparraguirre, K. R. Yang, S. S. Merchant, D. G. Truhlar, W. H. Green, *J. Am. Chem. Soc.* **2013**, *135*, 11100 – 11114.

[13] G. Knizia, T. B. Adler, H.-J. Werner, *J. Chem. Phys.* **2009**, *130*, 054104.

[14] We use DFT geometry optimization and frequency calculation at the B3LYP/6-311G(d) level of theory, as well as CCSD(T) single-point energies using explicit treatment of electron correlation (F12 method). Full details are provided in the Supporting Information.

[15] A mechanism involving initial associative displacement of CO by solvent (toluene) leading to an $[HCo(CO)_3(toluene)]$ complex, which itself undergoes substitution by the alkene, is the most promising such mechanism but the TSs are extremely hard to locate precisely. Our present calculations predict this route to be disfavoured over the dissociative route **1**–**3**–**4** but further work is needed to check whether such alternative mechanisms can play a role, especially at lower temperatures.

[16] a) J. N. Harvey, J. Jover, G. C. Lloyd-Jones, J. D. Moseley, P. Murray, J. S. Renny, *Angew. Chem.* **2009**, *121*, 7748 – 7751; *Angew. Chem. Int. Ed.* **2009**, *48*, 7612 – 7615; b) C. L. McMullin, J. Jover, J. N. Harvey, N. Fey, *Dalton Trans.* **2010**, *39*, 10833 – 10836; c) J. Jover, N. Fey, M. Purdie, G. C. Lloyd-Jones, J. N. Harvey, *J. Mol. Catal. A* **2010**, *324*, 39 – 47.

[17] J. W. Rathke, R. J. Klingler, T. R. Krause, *Organometallics* **1992**, *11*, 585 – 588.

[18] T. F. Hughes, J. N. Harvey, R. A. Friesner, *Phys. Chem. Chem. Phys.* **2012**, *14*, 7724 – 7738.

[19] According to NIST gas-phase thermochemistry data (http://webbook.nist.gov/chemistry/), $\Delta_f H$ for CO, C_3H_6, C_3H_8 and *n*-butyraldehyde is −110.53, 20.41, −104.7, and −204.4 kJ mol^{-1}, respectively.

[20] See for example, S. Kozuch, S. Shaik, *Acc. Chem. Res.* **2011**, *44*, 101 – 110.

[21] M. W. George, M. B. Hall, O. S. Jina, P. Portius, X.-Z. Sun, M. Towrie, H. Wu, X. Z. Yang, S. D. Zaric, *Proc. Natl. Acad. Sci. USA* **2010**, *107*, 20178 – 20183.

[22] K. J. Laidler, *Chemical Kinetics*, *3rd ed.*, Harper & Row, New York, **1987**.

[23] A. H. Krall, J. V. Sengers, J. Kestin, *J. Chem. Eng. Data* **1992**, *37*, 349 – 355.

[24] For the values of p_{H2} used in catalysis, the present model in fact predicts that the equilibrium between **1** and **23** is more evenly balanced.

